


Establishment and characterization of patient-derived organoids from a young patient with cervical clear cell carcinoma

Yoshiaki Maru¹ | Naotake Tanaka² | Keiko Ebisawa² | Akiko Odaka³ |
Takahiro Sugiyama³ | Makiko Itami³ | Yoshitaka Hippo¹ 

¹Department of Molecular Carcinogenesis, Chiba Cancer Center Research Institute, Chiba, Japan

²Department of Gynecology, Chiba Cancer Center, Chiba, Japan

³Division of Surgical Pathology, Chiba Cancer Center, Chiba, Japan

Correspondence

Yoshitaka Hippo, Department of Molecular Carcinogenesis, Chiba Cancer Center Research Institute, Chiba, Japan.

Email: yhippo@chiba-cc.jp

Funding information

Japan Society for the Promotion of Science, Grant/Award Number: 17K19624, 18K16823 and 19K09816

Abstract

Cervical clear cell carcinoma (cCCC) constitutes an extremely rare subtype of cervical cancer. Consequently, its pathogenesis remains largely unknown, with no cell lines established from primary tumors. Here, we report the first establishment of cCCC organoids, from biopsy samples of a 23-year-old patient diagnosed with cCCC. By applying a protocol that we recently optimized for gynecological tumors, we were able to propagate a patient-derived cell line (PDC) for more than 6 months as organoids. This PDC tolerated cryopreservation and proliferated either as spheroids or adherent cells, and developed xenografts in immunodeficient mice, ensuring robust utility as a cell line. Intriguingly, the resected tumor focally contained serous carcinoma (SC) in a tiny protruding lesion. Both organoids and derivative xenografts resembled the CCC component of the original tumor in histology, immunostaining profile, and genome-wide copy number changes, including focal gain of *MET*. Genomic analysis revealed that both organoids and the CCC component harbored only a few mutations, of which 2 mutations were shared in common. In contrast, the SC component showed a mutator-phenotype and prominent genome instability along with biallelic inactivation of *TP53*, but none of them were found in organoids or the CCC component. The PDC proved sensitive to major chemotherapeutic agents and *MET* inhibitors. These observations clearly indicated that the PDC, designated as YMC7, can be used as a novel cCCC cell line and provide novel insights into the pathogenesis of mixed cervical adenocarcinoma. As a valuable resource for rare cancer, it will likely contribute to investigations in many fields.

KEYWORDS

cervical cancer, clear cell carcinoma, organoid, patient-derived cell, preclinical model

Abbreviations aCGH, array-based comparative genomic hybridization; cCCC, cervical clear cell carcinoma; DES, diethylstilbestrol; FFPE, formalin-fixed paraffin-embedded; HPV, human papillomavirus; IHC, immunohistochemical; LOH, loss of heterozygosity; MBOC, Matrigel bilayer organoid culture; NGS, next-generation sequencing; oHGSC, ovarian high-grade SC organoid; PDC, patient-derived cell; pERK, phosphorylated ERK; SC, serous carcinoma; SNV, single nucleotide variant; VAF, variant allele frequency.

This is an open access article under the terms of the Creative Commons Attribution-NonCommercial-NoDerivs License, which permits use and distribution in any medium, provided the original work is properly cited, the use is non-commercial and no modifications or adaptations are made.

© 2019 The Authors. *Cancer Science* published by John Wiley & Sons Australia, Ltd on behalf of Japanese Cancer Association.

1 | INTRODUCTION

Cervical cancer has been a global threat to women's health. More than two-thirds of cervical cancers are classified as squamous cell carcinoma,¹⁻³ which is currently decreasing owing to intensive cervical screening and vaccination against HPV. The remainder are predominantly adenocarcinoma, which is on the rise worldwide, requiring prompt and practical measures against this disease. Cervical clear cell carcinoma is an extremely rare subtype of adenocarcinoma. It is histologically characterized by clear cytoplasm of cancer cells, closely resembling the features of its ovarian counterpart.⁴ Due to the small number of cases, epidemiological, clinical, and pathological features of cCCC have remained largely unknown.⁵⁻⁹ Limited information thus far reported includes that patients with cCCC at an advanced stage had poor prognosis,¹⁰ and that in utero exposure to the antimiscarriage drug DES and HPV infection might be implicated in its pathogenesis.¹¹⁻¹⁴ There are virtually no resources available for cCCC research either, such as genetically engineered mouse models, PDCs, or patient-derived xenografts. These situations make it yet more difficult to undertake research on cCCC.

Organoid culture is an emerging technique that enables infinite expansion of murine and human normal stem cells.^{15,16} To date, it has been applied to various research fields, including infectious disease models,¹⁷ developmental biology,¹⁸ and epithelial regeneration.¹⁹ We also reported the establishment of murine organoid-based carcinogenesis models for intestine,²⁰ lung,²¹ hepatobiliary tract,²² and pancreas.²³ These organoid culture techniques have now become common for patient-derived samples from diverse types of cancer, which revealed that tumor-derived organoids basically retained the morphology and genetic aberrations of the original tumors.²⁴⁻²⁶ Although its validity in gynecologic tumors has long remained elusive,²⁷ we recently established an efficient culture method optimized for ovarian and endometrial tumors,²⁸ by modification of an MBOC protocol that we initially developed for a murine carcinogenesis model *ex vivo*.²⁹

In an effort to systematically collect various gynecologic tumors as PDC, we experienced a case of cCCC. Based on its scarcity, we dared to undertake its organoid culture using our new modified protocol, although we had never cultured primary cervical adenocarcinoma before. In this study, we successfully propagated and characterized tumor-derived organoids, establishing a novel cell line that basically retained the features of the original tumor. This PDC will likely provide mechanistic insights into cCCC and serve as a promising resource for preclinical studies.

2 | MATERIALS AND METHODS

2.1 | Patient information

This study was approved by the Ethics Committee of Chiba Cancer Center (Chiba, Japan) with Institutional Review Board approval number H28-J158. Written informed consent was obtained from the patient. The detailed clinical information will be submitted elsewhere as a case report (K. Ebisawa, M. Ijiri, K. Suzuka, T. Sugiyama, M. Itami, N. Tanaka, unpublished data.). Briefly, the patient was a 23-year-old woman without infection with the 13 strains of high-risk HPVs. Radical hysterectomy with bilateral adnexectomy and pelvic lymphadenectomy were carried out for the cervical tumor. The resected tumor was histologically diagnosed with pT1b2N0M0. The patient was treated with adjuvant chemotherapy by irinotecan hydrochloride and nedaplatin. No obvious signs of recurrence have been detected at our outpatient department for 6 months after surgery.

2.2 | Isolation of tumor cells and primary organoid culture

The biopsy samples were minced and dissociated into small clusters or single cells by digesting with 2 U/mL dispase II, 1 mg/mL collagenase P (Roche Diagnostics, Tokyo, Japan) and Accumax (Innovative Cell Technologies, San Diego, CA, USA). The resuspended cells were plated on solidified Matrigel (BD Biosciences, Franklin Lakes, NJ, USA). The following morning, viable cells attached to Matrigel were covered with Matrigel and overlaid with media to start the organoid culture. To increase the yield of tumor cells, we further carried out digestion of floating tissue fragments and cell aggregates by Accumax treatment and then undertook organoid culture. Primary organoid culture was carried out according to the modified MBOC protocol as previously described²⁸ and in Data S1.

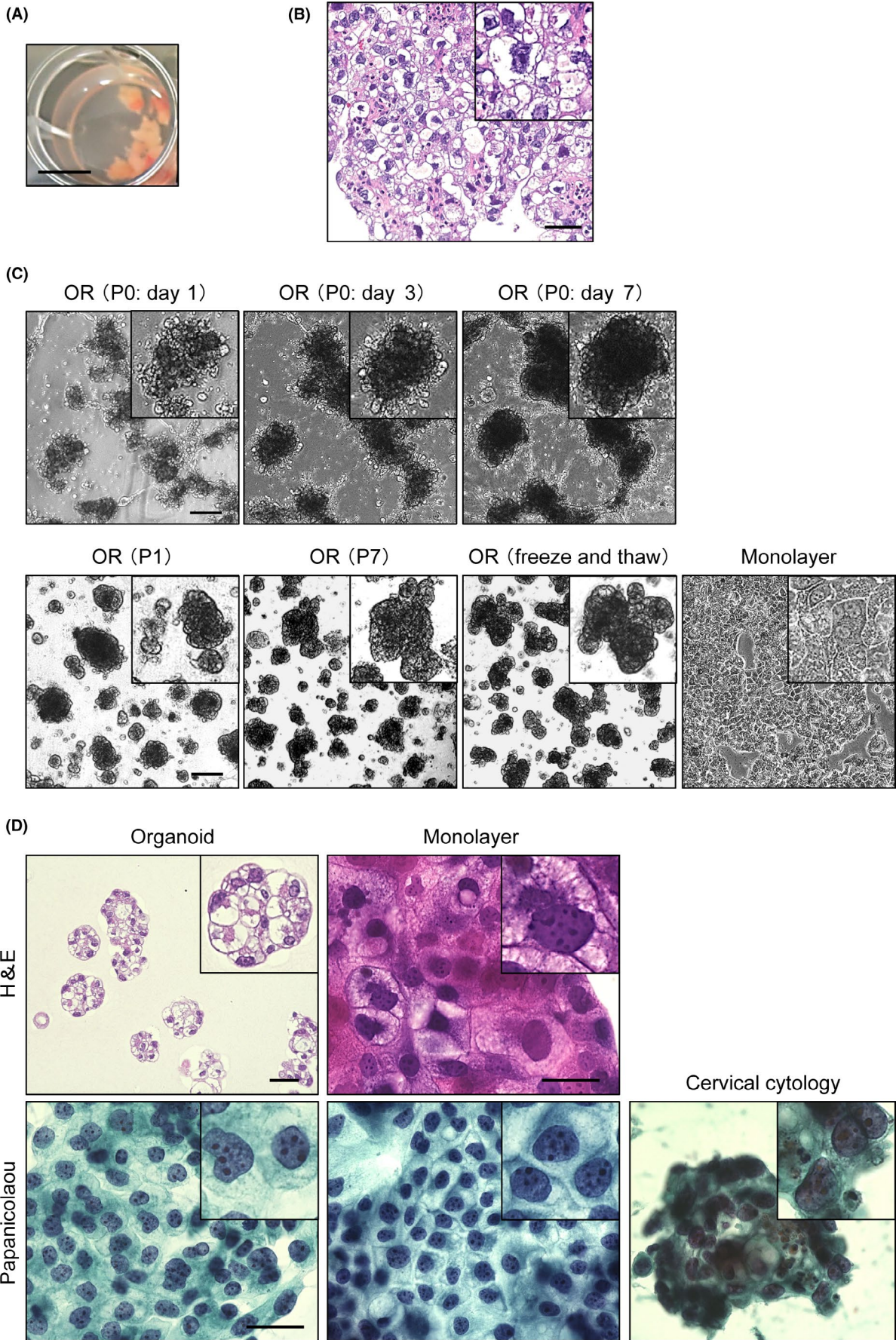
2.3 | Pathological analysis

Organoids obtained by depolymerization of Matrigel with Cell Recovery Solution (BD Biosciences) were resuspended in iPGell (GenoStaff, Tokyo, Japan). The iPGell-embedded organoids or resected tumors were fixed in 10%-15% buffered neutral formalin, dehydrated, and embedded in paraffin. The detailed methods are described in Data S1.

2.4 | Genomic DNA analysis

NucleoSpin Tissue (Takara, Shiga, Japan) and a QIAmp DNA FFPE Tissue Kit (Qiagen, Hilden, Germany) were used for extraction

FIGURE 1 Stable propagation of cervical clear cell carcinoma-derived organoids by modified Matrigel bilayer organoid culture. A, Biopsy sample collected from the cervical tumor. Scale bar = 10 mm. B, H&E staining of biopsy sample. Scale bar = 50 μ m. Inset shows a magnified image. C, Upper panels, representative time-lapse images of tumor-derived organoids (OR) in the bright field (passage [P]0) at 1-7 d. Lower panels, organoids after P1 and P7 and recovered from a cryopreserved sample. Adherent cells growing in monolayer are also shown. Scale bar = 200 μ m. Insets show magnified images. D, Pathological examination of organoids (left) and organoid-derived adherent cells (middle). Upper panels, H&E staining. Lower panels, Papanicolaou staining. Cervical cytological specimens are shown as a reference (right). Scale bar = 50 μ m



of genomic DNA from organoids and FFPE samples of tumor and normal tissues, respectively, and subjected to NGS analysis as previously described,³⁰ and aCGH analysis. The detailed methods are described in Data S1.

2.5 | Tumorigenicity assay

Immunodeficient nude mice BALB/cA^{nu/nu} were purchased from CLEA Japan (Tokyo, Japan). Animal studies were carried out with the approval of the Chiba Cancer Center for Ethics in Animal Experimentation. Tumor-derived organoids corresponding to 5×10^5 cells were resuspended in 100 μ L advanced DMEM/F12 mixed with 100 μ L Matrigel at a 1:1 ratio and inoculated into one side of the dorsal skin of nude mice. Tumor development was monitored for 3 months.

2.6 | Cell proliferation and drug sensitivity assay

For in vitro assay, organoids were collected and dissociated into single cells by digesting with Accumax. The dissociated cells were counted using a TC20 Automated Cell Counter (Bio-Rad, Hercules, CA, USA). For cell proliferation assays, 2×10^4 single cells/well were plated in a 24-well plate with solidified Matrigel to form organoids, or an ultra-low attachment 24-well plate to generate spheroids. Cell viability was analyzed with CellTiter-Glo3D Cell Viability Assay (Promega, Fitchburg, WI, USA) at 5 time points (day 0, 3, 7, 10, and 14) in triplicate, and the results were normalized to the values on day 0. For the drug sensitivity assay, 5×10^3 single cells/well were plated into PrimeSurface 96U (Sumitomo Bakelite, Tokyo, Japan) in triplicate. At 48 hours after plating, paclitaxel (Wako, Osaka, Japan), cisplatin (Wako), gemcitabine hydrochloride (Wako), crizotinib (Tocris Bioscience, Bristol, UK), and SU11274 (Cayman Chemical, Ann Arbor, MI, USA) were dispensed at 5 serially diluted doses from 5 to 100 nmol/L, from 1 to 100 μ mol/L, from 1 to 100 nmol/L, from 100 nmol/L to 10 μ mol/L and, from 100 nmol/L to 10 μ mol/L, respectively, and analyzed in triplicate following 96 hours of drug incubation. The mean \pm SD of the results from 3 independent experiments is shown for each drug.

3 | RESULTS

3.1 | Propagation of organoids from a cervical biopsy sample of CCC

In order to expand patient-derived organoids of cCCC, we obtained a biopsy sample (Figure 1A) from a female patient diagnosed with cCCC. We first evaluated one-third of the samples by histological analysis and confirmed that cancer cells manifested nuclear atypia and clear cytoplasm, consistent with general features of CCC (Figure 1B). The rest were subjected to primary organoid culture with the modified MBOC protocol.²⁸ Following dissemination on solidified Matrigel and with serum-free organoid culture media,

organoids readily formed small or large solid structures with multiple budding, which was sustained after embedding in Matrigel and over serial passages (Figure 1C). We also confirmed that cCCC-derived organoids could be propagated for at least 6 months, tolerated a cycle of freeze and thaw, and proliferated as a monolayer for at least 2 months in the absence of Matrigel (Figure 1C).

To examine to what extent propagated organoids retained the features of the original tumor, we histologically compared organoids and the biopsy specimen by H&E staining of FFPE sample-derived thin sections. Organoids exclusively consisted of atypical cells with clear cytoplasm (Figure 1D), concordant with morphological features of the original tumor (Figure 1B). Similar results were obtained for monolayer cells (Figure 1D). We also made a comparison by using Papanicolaou staining, a routine procedure in cytological examination. Again, we confirmed that cells within organoids and in monolayer resembled the original malignant cells detected in cervical cytological specimens for the initial diagnosis (Figure 1D).

3.2 | Retention of histological features of CCC component, but not SC component, in biopsy-derived organoids

While we were characterizing the biopsy-derived organoids, the patient underwent surgery. The cervical tumor with exophytic papillary growth was resected, which was as large as 5.0 cm \times 3.0 cm \times 4.0 cm (Figure 2A). The tumor showed papillary structures with fibrous stalks (Figure 2B). Intriguingly, the lesion at the peripheral tip, comprising 5% of the tumor, showed histological features quite distinct from the rest (Figure 2B). High-magnification observation revealed that the majority of cancer cells showed nuclear enlargement, irregular nuclei, and clear cytoplasm, consistent with the diagnosis of CCC (Figure 2C) and the histological features of the biopsy sample (Figure 1B). However, the minor fraction proved to be SC, another rare subtype of cervical adenocarcinoma (Figure 2C).

To verify that the biopsy-derived organoids indeed derived from the CCC component of the original tumor, we set out to undertake IHC analysis. We selected multiple markers widely used to distinguish between CCC and SC.³¹ Specifically, HNF1- β , Napsin A, ARID1A, and p53 were evaluated. The CCC cells of the original tumor were positive for HNF-1 β as predicted, but also positive for ARID1A and negative for Napsin A, unlike typical ovarian CCC. Accumulation of p53 was evident in CCC, but its expression level varied within the CCC area (Figure 2C). These results suggest that this cCCC case might be only partially similar to typical ovarian CCC in terms of histological features. In contrast, SC cells of the original tumor showed strongly positive for p53 and ARID1A, but not for HNF-1 β , or Napsin A, compatible with the typical phenotype of ovarian SC (Figure 2C). We also confirmed that both organoids and the original tumor had high expression of Ki-67, indicative of active proliferation (Figure 2C). Collectively, these observations suggested that the organoids were likely derived from the CCC component, but not from the SC component.

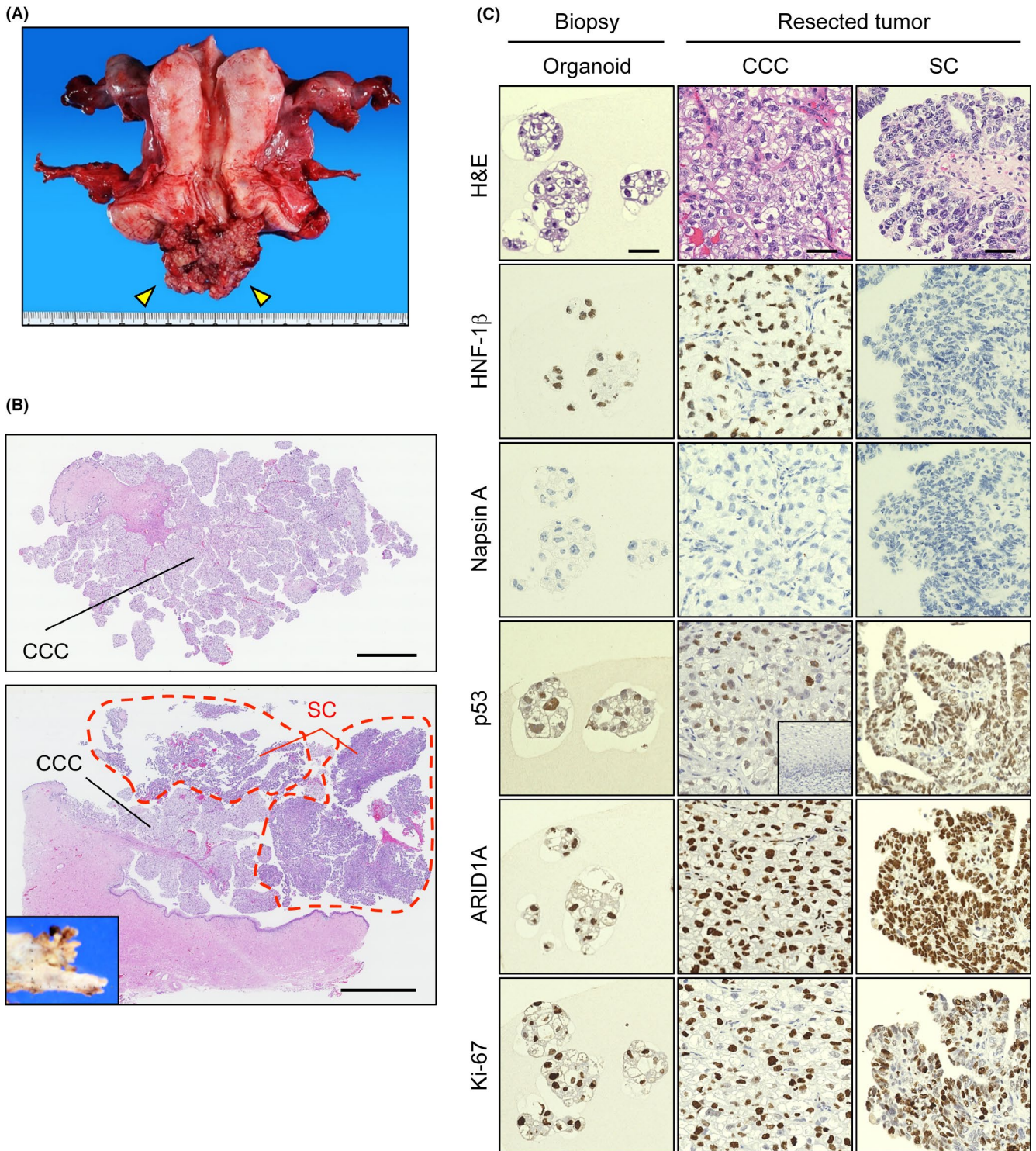


FIGURE 2 Histological characterization of the tumor with clear cell carcinoma (CCC) and serous carcinoma (SC) components. A, Macroscopic view of a resected cervical tumor (arrowheads) at the bottom of the uterus. B, Whole slide images of the cervical tumor stained with H&E. Upper panel, thin section of tumor homogeneously occupied by papillary growing CCC. Lower panel, thin section of tumor with mixed histology. CCC component was placed in the proximal part; SC component occupied peripheral lesions (circles). Inset shows a macroscopic view of the corresponding part of the formalin-fixed tumor. Scale bar = 5 mm. C, Histological examination by H&E and immunohistochemical staining. Left, biopsy-derived organoids. Middle, CCC component of the tumor. Right, SC component of the tumor. An inset for p53 staining in CCC shows the result of staining in normal cervical mucosa as a reference. Scale bar = 50 μ m

3.3 | Retention of original CCC histological features in organoid-derived xenograft

To further verify the CCC origin of the biopsy-derived organoids, we inoculated the organoids at passage 3 (Figure 3A) into the bilateral dorsal skin of nude mice. Initially, it appeared that a palpable tumor developed only on the right side (Figure 3B). However, a tiny nodule on the left side was later found at the time of death (Figure 3C). The cut surface of the right tumor indicated that it had indeed a solid nature (Figure 3D). Microscopic analysis by H&E staining revealed that both the nodules contained papillary and solid fractions (Figure 3E). Precise histological evaluation showed that both nodules were predominantly composed of cancer cells with nuclear atypia and clear cytoplasm (Figure 3F), strongly resembling the histological properties of the organoids and the original CCC (Figure 2C). Immunohistochemical analysis also indicated that protein expression profiles in both nodules were significantly similar, including positive findings in HNF1- β , p53, and Ki-67 (Figure 3F). Based on these findings, we concluded that the organoids were highly likely to consist of a pure cCCC population and retain the original features of the tumor. The right s.c. tumor was recovered as cCCC organoids, which remained almost the same in morphology to those before inoculation (Figure 3G). To confirm the reproducibility of the xenograft development from organoids, we tried inoculation of organoids again at passage 7. However, no s.c. tumor developed, even after 3 months. These observations suggest that the biopsy-derived CCC organoids might have only low tumorigenic potential, which was further lowered during culture by unknown mechanisms.

3.4 | Retention of original CCC genetic aberrations and heterogeneity in biopsy-derived organoids

In many types of cancers, it has been reported that tumor-derived organoids basically retained the majority of somatic mutations, copy number variations, and intratumoral heterogeneity observed in the original tumors.³²⁻³⁴ To verify this notion in this case, we compared the biopsy-derived organoids and FFPE samples of the original tumor's CCC component at the genome level, by targeted sequencing analysis of 409 cancer-related genes. Organoids and original CCC harbored only 4 and 3 mutations, respectively, of which 2 mutations were shared in common (Figure 4A). These were a nonsynonymous mutation in *MLH1* and a synonymous mutation in *TFE3*. The VAF for

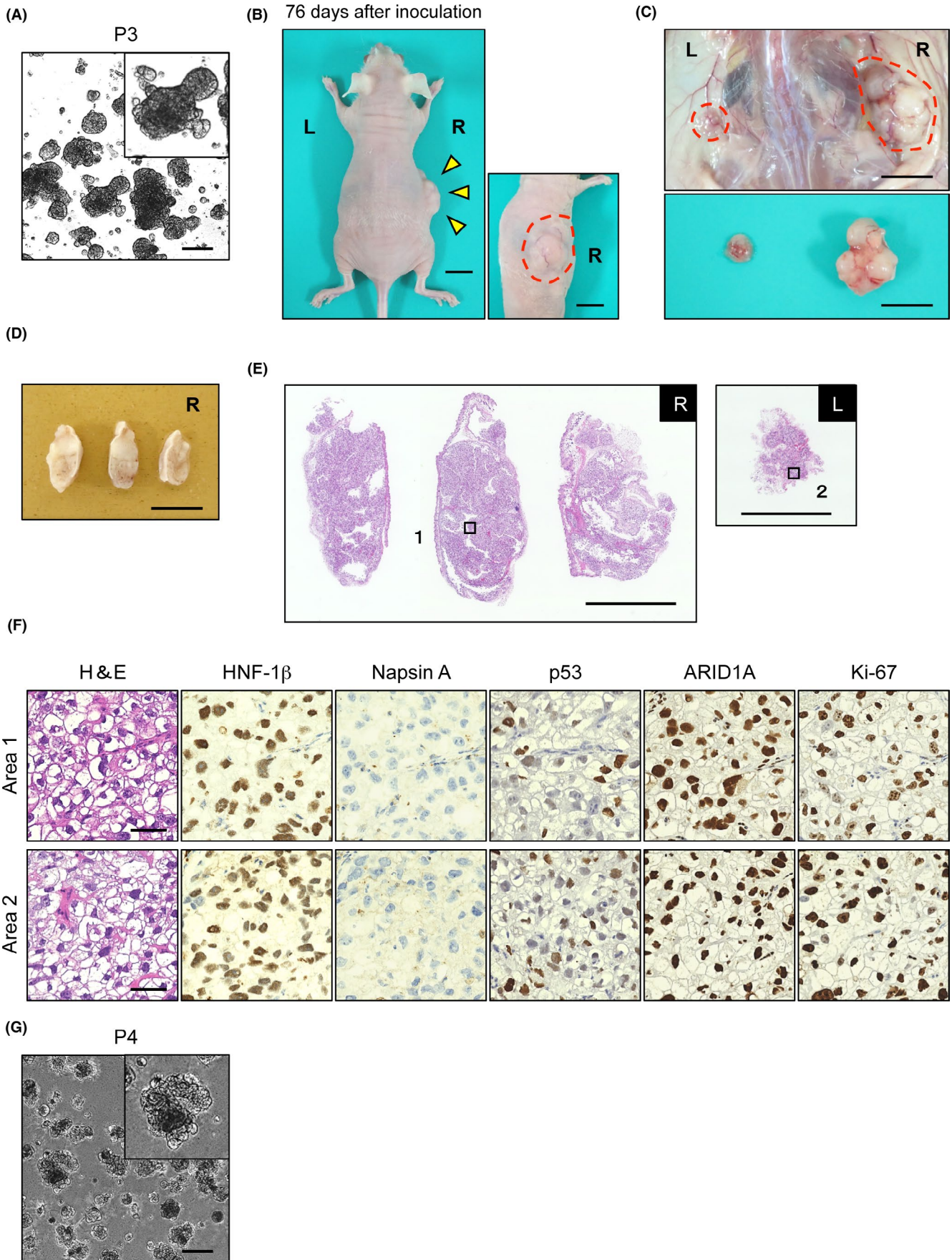
TFE3 was 37% in organoids and 49% in the original CCC (Figure 4A). Being a synonymous mutation, it is unlikely that the *TFE3* mutation was positively selected among cancer cells during culture. In addition, VAF of the *TFE3* mutation was almost 50% in organoids, strongly suggesting that cancer cells in the tumor might purely consist of heterozygous mutant cells, which selectively propagated as organoids, leading to a 1.32-fold enrichment of cancer cells. The VAF for the *MLH1* mutation increased by 1.37-fold from 30% in CCC to 41% in organoids (Figure 4A), suggestive of a similar magnitude of enrichment of cancer cells. The VAF of the mutant allele at 41% theoretically predicts that heterozygous mutant cells and WT cells would comprise 82% and 18%, respectively, indicative of the heterogeneity in organoids.

In contrast, the original SC harbored a large number of mutations. However, no shared mutations with organoids or the CCC component were identified, unequivocally revealing their distinct natures (Figure 4A). Notably, the SC component harbored multiple nonsynonymous mutations in DNA repair-related genes, including *PARP1*, *FANCD2*, and *PMS2* (Table S1). Hence, it is possible that defects in DNA repair underlie the observed mutator phenotype in the original SC. Based on the NGS data, we also estimated genome-wide copy number changes in these samples. Although the signal to noise ratio of the data was relatively low, it seemed likely that the copy number gain in *MET* and the genome-wide copy number changes were shared by organoids and the original CCC, but not by the original SC (Figure 4B).

3.5 | Serous carcinoma-specific microdeletion and biallelic inactivation of *TP53*

It has been well established that *TP53* is almost invariably mutated in ovarian high-grade SC.³⁵ Together with the observation that p53 was accumulated in the original SC, and to a lesser extent in the original CCC (Figure 2C), we assumed that the tumor would likely harbor a *TP53* mutation. However, NGS analysis did not uncover point mutations in *TP53*. We then carefully examined the raw NGS data for the *TP53* gene, and found a 3-bp in-frame deletion (c.754_756 del CTC) exclusively in SC (Figure 4C), which could result in p53 accumulation in tumors.³⁶ Interestingly, we found a heterozygous SNV at c.215 (C > G), which results in amino acid substitution from Pro to Arg at codon 72 (Figure 4D). This particular situation allowed us to distinguish between the 2 alleles of *TP53*. The VAF of the WT allele at this nucleotide was approximately 50% in all the samples except for 10% in the SC component. As a tumor suppressor frequently

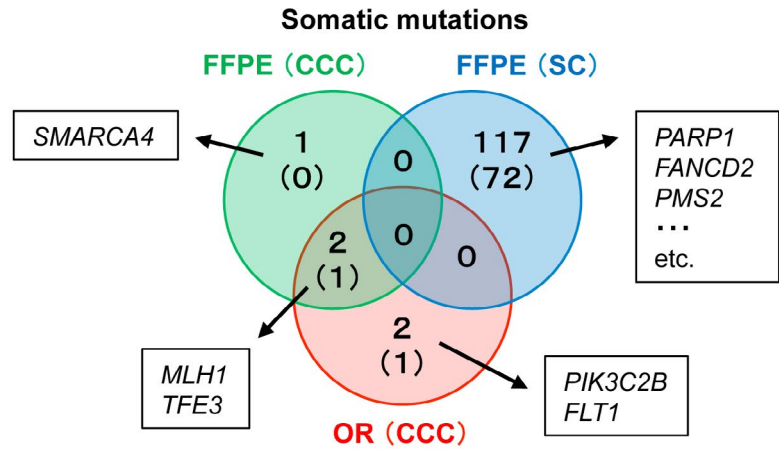
FIGURE 3 Development of xenograft from cervical clear cell carcinoma organoids. A, Bright field image of organoids before inoculation in nude mice (passage [P]3). Scale bar = 200 μ m. Inset shows a magnified image. B, Palpable tumor development in nude mice. Mice were killed 76 days after duplicate inoculation of tumor organoids on both left (L) and right (R). Left image, whole body image from the back. A solid tumor was evident only on the right side (arrowheads). Right image, lateral view of the tumor. The tumor consisted of multiple nodules (circle). Scale bar = 10 mm. C, Isolated tumors. Upper panel, macroscopic views of the tumors on both sides (circle) during dissection. Lower panel, isolated tumors. Scale bar = 10 mm. D, Slices of tumor after formalin fixation. Scale bar = 10 mm. E, Whole slide images of the right tumor and left nodule stained with H&E. Right solid tumor was sliced into 3 pieces. The 2 boxes show areas magnified in (F). Scale bar = 5 mm. F, Comparison of histopathological features between left tiny nodule and right solid tumor by H&E and immunohistochemical staining against HNF-1 β , Napsin A, p53, ARID1A, and Ki-67. Scale bar = 50 μ m. G, Bright field image of s.c. tumor-derived organoids (P4). Inset shows a magnified view. Scale bar = 200 μ m



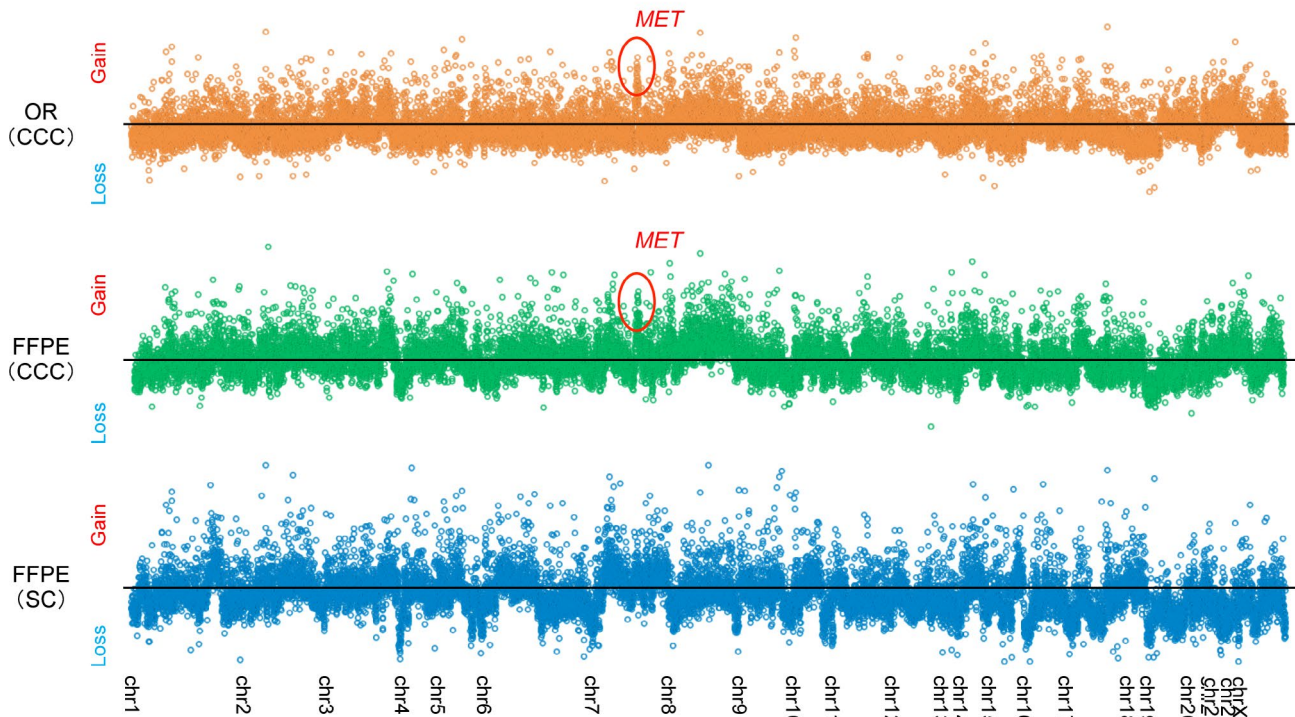
(A)

FFPE (CCC) and OR (CCC)

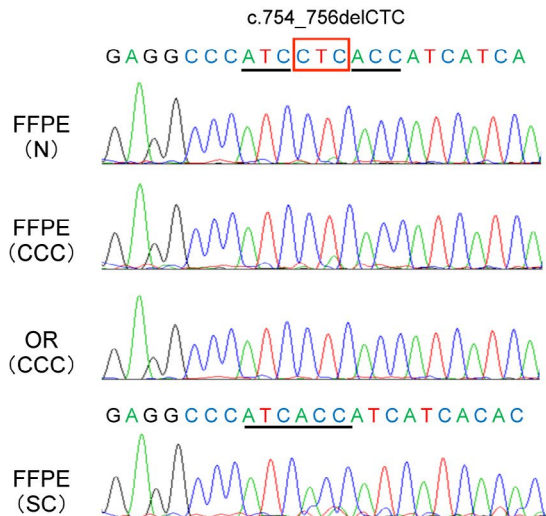
| Gene | S/N | VAF (%) | |
|----------------|-----|---------|----|
| | | FFPE | OR |
| <i>PIK3C2B</i> | N | 0 | 13 |
| <i>MLH1</i> | N | 30 | 41 |
| <i>FLT1</i> | S | 0 | 14 |
| <i>SMARCA4</i> | N | 28 | 0 |
| <i>TFE3</i> | S | 37 | 49 |



(B)



(C)



(D)

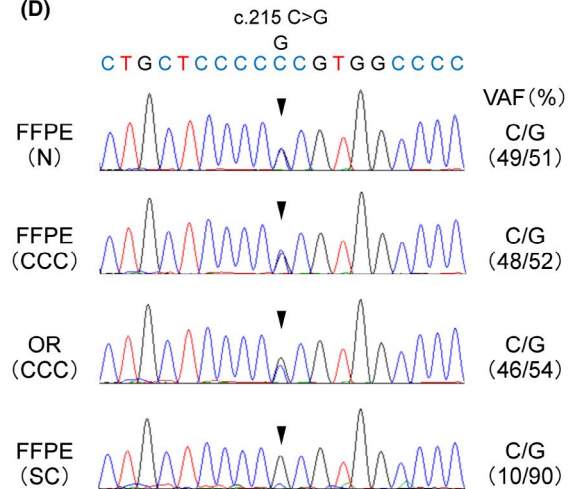


FIGURE 4 Mutation profiles of cancer-related genes in biopsy-derived organoids and the resected original tumor. A, Mutation profiles by target sequence analysis. Left, a list of somatic mutations in clear cell carcinoma (CCC) component (formalin-fixed paraffin-embedded [FFPE]) and biopsy-derived organoids (OR). N, nonsynonymous mutation; S, synonymous mutation. Right, Venn diagram of somatic mutations in CCC and serous carcinoma (SC) component and biopsy-derived organoids. The numbers in parentheses indicate the number of synonymous mutations. B, Estimation of copy number alterations based on depth of coverage obtained using targeted sequencing of 409 cancer-related genes. Focal amplification at the *MET* locus was implied in organoids and CCC component of the tumor. C, Validation of an SC component-specific in-frame 3-base deletion (box) in the *TP53* gene (c.754_756del CTC) by Sanger sequencing. D, Validation of a germ-line heterozygous single nucleotide variant in the *TP53* gene (c.215 C>G) (arrowheads) by Sanger sequencing. VAF, variant allele frequency

inactivated by LOH, we predicted the presence of *TP53* LOH in SC, but it was difficult to confirm 1 copy loss from the putative copy number inferred from the NGS data.

We then set out to accurately measure copy number alterations by aCGH analysis. The FFPE samples of CCC organoid-derived xenograft and the tumor's CCC and SC components were compared. The copy number alterations of the xenograft were similar to those of the original CCC, with further accumulation of alterations in xenograft (Figure 5A). Specifically, we found chromosomal gain at 8 and 22, and loss at 13, 18, and 21 in common. In sharp contrast, the genomic copy number of SC was significantly altered. As predicted, 1 copy loss of *TP53*, along with whole chromosome 17p, was observed in SC (Figure 5A).

3.6 | Clear cell carcinoma-specific overexpression of *MET*

Copy number gain of *MET* in CCC and xenograft, but not in SC, was also confirmed by aCGH (Figure 5A). To investigate whether and in what proportion *MET* is overexpressed, we undertook IHC staining. Membranous staining of *MET* was observed in the CCC, organoids, and xenograft, but not SC or normal cervix (Figure 5B). Notably, *MET* overexpression was unanimously observed in these CCC-related samples, suggesting its critical roles in CCC development. As MEK/ERK and PI3K/AKT pathways are the major pathways downstream of *MET*, we further analyzed the status of AKT and ERK by IHC staining. There were pERK-positive cells in CCC-related samples, but the majority of cells with *MET* overexpression were not positive for pERK (Figure 5B). On the contrary, SC rather contained more pERK-positive cells than did CCC despite *MET* overexpression. Moreover, pAKT was not detected in either SC or CCC-related samples (Figure 5B). These results suggest that *MET* might exert its pro-oncogenic effects through noncanonical pathways in this CCC case.

3.7 | Drug sensitivity of cCCC organoid-derived spheroids for anticancer drugs

For high-throughput drug screening, Matrigel-based organoids might not be ideal, as time-consuming and complicated procedures are usually required. Practically, spheroids and adherent cells are more favored. In this regard, we previously confirmed that organoids from ovarian and endometrial tumors could generally be turned into spheroids, and used for drug-sensitivity assay.²⁸ In a similar manner, we dissociated cCCC organoids into single cells and split them into organoid and spheroid cultures. Cells readily aggregated and developed large

spheroids, in a comparable way to organoids in Matrigel (Figure 6A). We noted that organoids and spheroids proliferated comparably at least for 1 week from the beginning of the culture (Figure 6B). Based on these observations, we reasoned that spheroid-based drug sensitivity assay would mimic similar responses to organoids, if carried out within 7 days. We then treated cCCC organoids with anticancer drugs commonly used in clinic for gynecological cancer. The IC_{50} values for paclitaxel and cisplatin were 20 nmol/L and 19 μ mol/L, respectively (Figure 6C), which were comparable to IC_{50} values of ovarian cancer organoids for paclitaxel (10–100 nmol/L) and cisplatin (10–100 μ mol/L), respectively.²⁸ The IC_{50} value for gemcitabine was 37 nmol/L, which was comparable to that of pancreatic cancer organoids (1–100 nmol/L).³⁷ Given that ovarian and pancreatic cancers are relatively sensitive to these agents, cCCC organoids would be likely sensitive to these drugs as well.

With amplification of the *MET* gene, we speculated that cCCC organoids would be sensitive to crizotinib, a clinically approved *MET* inhibitor, owing to a mechanism known as “oncogene addiction”. We included oHGSC that we recently established²⁸ as a negative control without *MET* amplification (Figure 6D), and investigated responses of these 2 organoids to crizotinib. Although cCCC organoids appeared to respond better than oHGSC organoids in the range of <1 μ mol/L, IC_{50} values of cCCC and oHGSC organoids were largely similar, with 2.2 μ mol/L and 1.3 μ mol/L, respectively (Figure 6D). As crizotinib potentially inhibits not only *MET* but also anaplastic lymphoma kinase, we reasoned that observed marginal difference in drug sensitivity might be attributable to anaplastic lymphoma kinase inhibition by crizotinib. We therefore tested SU11274, a specific *MET* inhibitor. The IC_{50} values of cCCC and oHGSC were 1.7 μ mol/L and >10 μ mol/L, respectively (Figure 6D). Considering that IC_{50} values of ES2 and RMG1, ovarian CCC cell lines with *MET* overexpression, were 5 μ mol/L and 3 μ mol/L, respectively,³⁸ it is likely that the cCCC organoids are sensitive to SU11274, and thereby suggestive of addiction to *MET*.

4 | DISCUSSION

In this study, we newly established a cell line from primary cCCC by organoid culture. Through detailed analyses of organoids and the original tumor, we confirmed that this PDC retained many features of the original cCCC, and can be subjected to drug screening in vitro as spheroids, and potentially in vivo as xenografts. We therefore designated the cell line as YMC7 for future distribution in the research community. To the best of our knowledge, this is the first successful

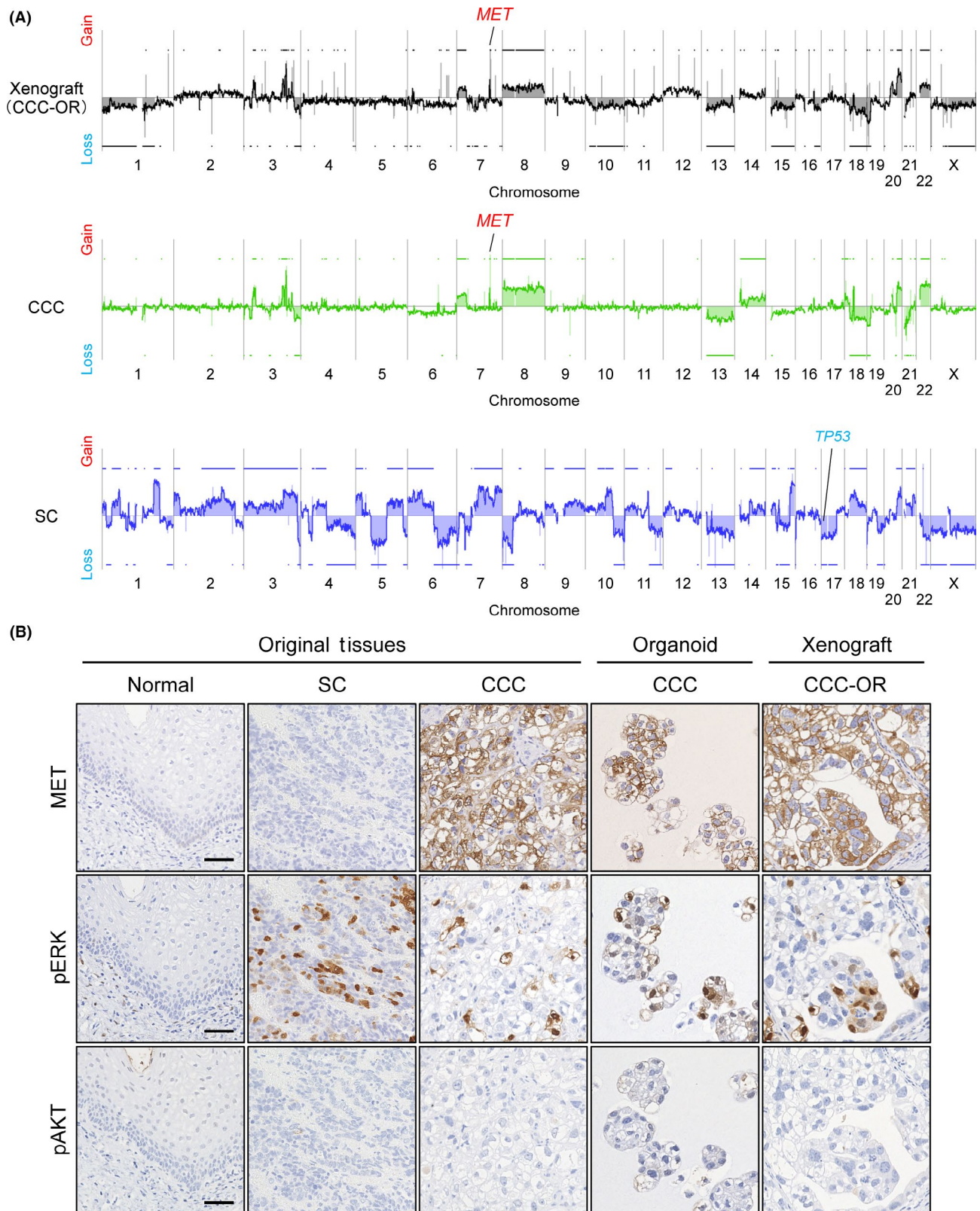
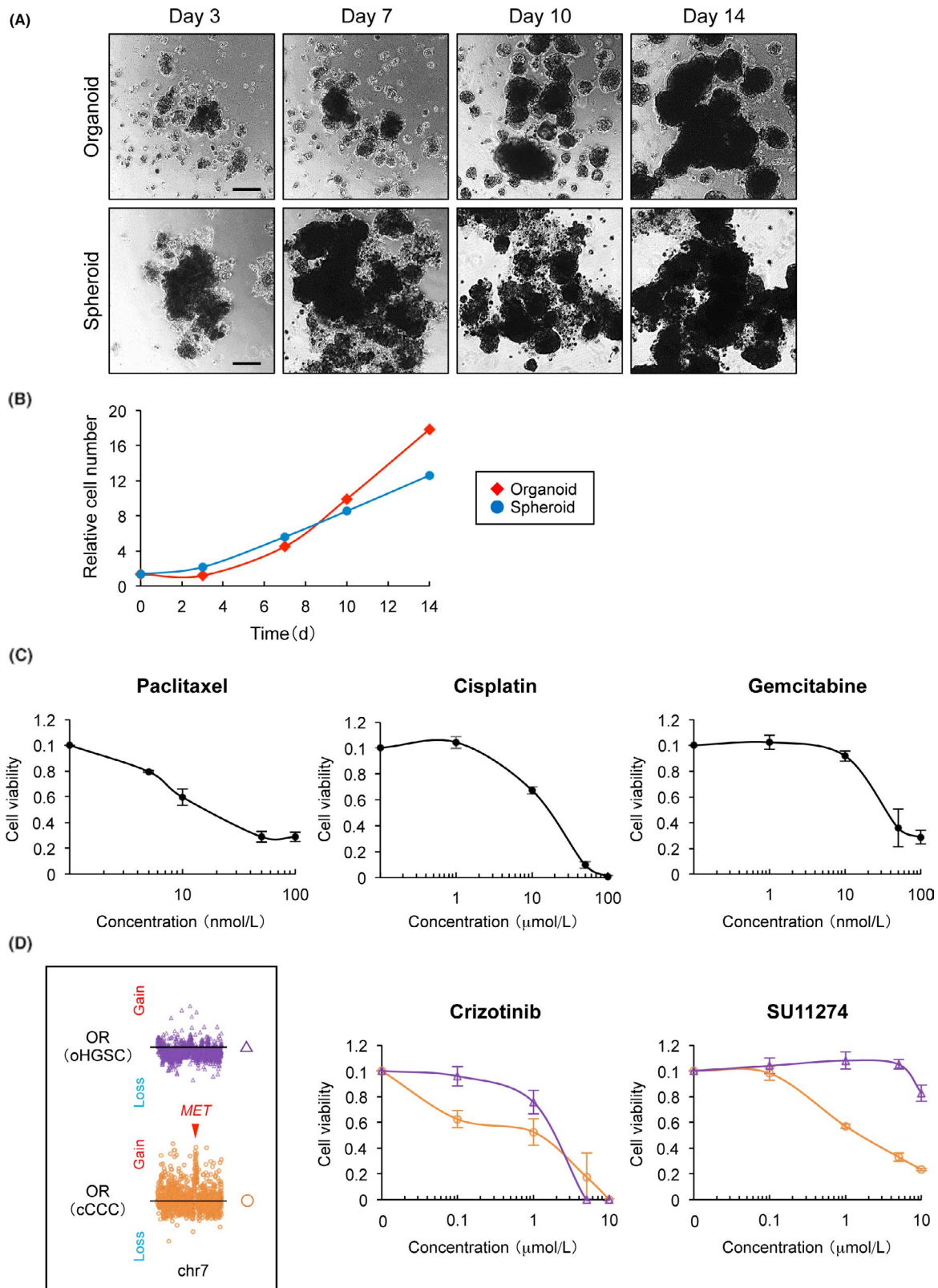


FIGURE 5 Retention of copy number alterations of original cervical clear cell carcinoma in organoid-derived (CCC-OR) xenograft. A, Copy number alterations of the original cervical tumor and organoid-derived xenograft. Formalin-fixed paraffin-embedded samples were analyzed. Focal copy number gain of *MET* in organoid-derived xenograft and CCC component of the tumor were detected. Serous carcinoma (SC) component showed extensive genomic instability, including a copy number loss of *TP53*. B, Immunohistochemical staining of *MET*, phosphorylated (p)ERK, and pAKT. Scale bar = 50 μ m



case of organoid culture of primary cervical adenocarcinoma, let alone cCCC. As an adherent cell line, only 1 case of cCCC was documented some 30 years ago.³⁹ Whereas this cell line with high tumorigenic potential was established from cancerous ascites of a dead patient, YMC7 derives from a resectable primary tumor in a young patient and shows low tumorigenic potential. Consequently, it could help investigations on the mechanisms underlying the early phase of carcinogenesis of cCCC, and recapitulation of tumor progression by gene transduction into organoids. Given the low number of studies with cCCC, we referred to studies in ovarian CCC,^{40,41} which is the second most common ovarian epithelial cancer in Japan.¹ For example, chromosomal gains and losses identified in cCCC resembled those of ovarian CCC previously documented.⁴² In addition, copy number gain of *MET* and protein overexpression of *MET* in cCCC were previously documented in ovarian CCC.^{43,44} These findings suggest that the mechanisms underlying carcinogenesis of cCCC might be highly correlated with those of ovarian CCC. As predicted, pharmacological *MET* inhibition potently impaired the growth of

cCCC cells, suggesting that the *MET* gene might have potential as a therapeutic target in case of recurrence of this cCCC.

Without an episode of DES exposure in utero or infection with high-risk HPV, this case might not be typical of cCCC of the young. Although the mechanisms underlying tumor development in this case remain largely unknown, there were some findings that could possibly account for such unusual onset. First, there was a somatic mutation in *MLH1* in this case. Lynch syndrome-related cCCC⁸ and POLE-mutated cCCC⁹ have been previously documented, in which mismatch repair genes including *MLH1* were commonly affected, leading to a mutator phenotype in these diseases. However, only a few mutations were identified in this cCCC case, suggesting that the *MLH1* mutation might not be relevant in carcinogenesis or could exert protumorigenic effects by unknown mechanisms. Second, early onset and low mutational burdens rather suggested that a fusion gene might underlie the carcinogenesis in this case. Hence, its exploration by RNA sequencing might be warranted. Finally, a heterozygous SNV in the *TP53* gene that gives rise to codon 72 polymorphisms (Pro > Arg) was identified. As one of the common polymorphisms (rs1042522), it is under

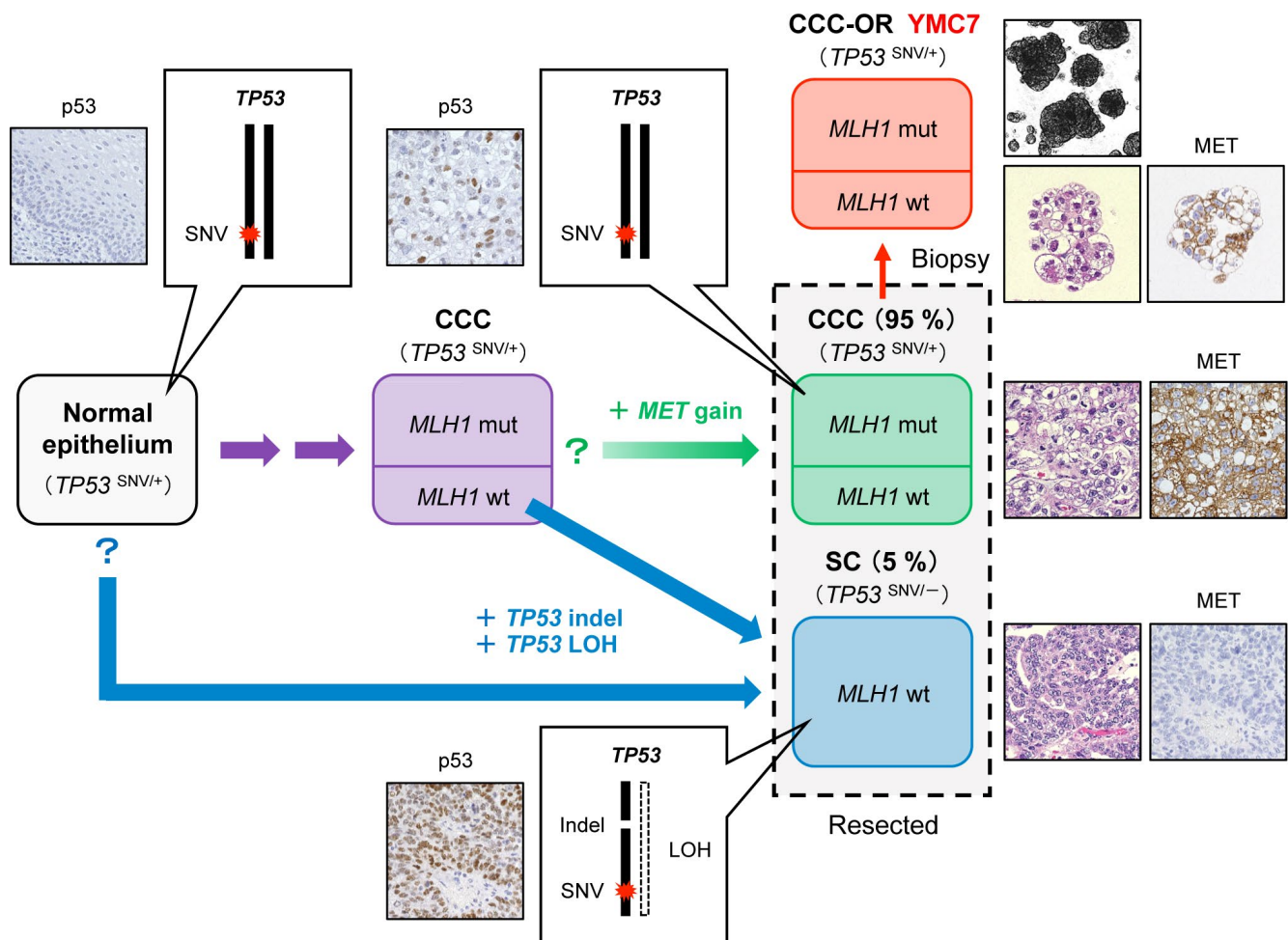


FIGURE 7 Possible mechanisms underlying the development of cervical adenocarcinoma with clear cell carcinoma (CCC) and serous carcinoma (SC) components. A putative model for bidirectional carcinogenesis of the cervix in this study. SC sequentially developed from a CCC-related common precursor. In this model, the timing of *MET* copy number gain remains elusive. Alternatively, it is also possible that the 2 components independently developed as a collision tumor, although its probability might not be high. LOH, loss of heterozygosity; mut, mutant; OR, organoid; SNV, single nucleotide variant

intensive investigation.⁴⁵ It has been reported that this polymorphism increased the risk of cancer in Asian and African Americans⁴⁶ and is more susceptible to degradation by the HPV 18 E6 protein,⁴⁷ raising the possibility that gynecological cancer in Japanese patients might be promoted by this polymorphism. However, it was shown that Arg72 variant p53 could induce apoptosis more efficiently than Pro72 variant p53.⁴⁸ As seen above, there are many inconsistencies on the functional roles of codon 72 polymorphisms of p53 across cancer types and ethnicities,⁴⁵ it makes it difficult to determine its exact roles. In this study, accumulation of p53 was observed in CCC but not in normal cervical mucosa, although they had the same genotype for TP53. It is tempting to speculate that this heterozygous SNV itself might not directly induce dysfunction of p53, but can cooperate with some cancer-related mutations, which is to be investigated further.

Another unusual aspect of this cCCC case is that it also contained a fraction of SC, another rare subtype of cervical adenocarcinoma. Both genomic and histological analyses clearly indicated the distinct nature of SC and CCC in the original tumor, strongly suggesting that they might have developed independently. However, intratumoral localization of the SC component was distal to the CCC component without direct connection with cervical tissue, rather suggesting its derivation from CCC in this case. It is well known that the TP53 gene is frequently mutated in ovarian high-grade SC³⁵ and endometrial SC.⁴⁹ In this study, we also identified a 3-bp in-frame deletion and LOH in the TP53 gene in the SC component of the tumor. Accumulation of p53 was also observed, consistent with the same 3-bp deletion in ovarian SC.³⁶ These observations suggest that aberration of the TP53 gene might be implicated in the carcinogenesis of cervical SC as well. Based on these findings, we now propose possible mechanisms underlying the development of this case with mixed-type cervical adenocarcinoma (Figure 7). In this model, CCC first occurred from cervical tissue of a patient with a heterozygous SNV in TP53 genes. The MLH1 gene was then mutated in a population that expanded to more than two-thirds of CCC cells. However, 3-bp deletion and LOH of the TP53 gene occurred in a fraction of CCC cells without mutated MLH1, and subsequently transformed into SC cells. The copy number gain of MET occurred in only CCC cells, although its timing remains undetermined. Another possibility is that both components occurred from distinct lesions of normal cervical epithelia in a completely independent manner, which is known as a collision tumor, although it is relatively rare in gynecological tumors.⁵⁰

In conclusion, we established a novel cell line of an extremely rare gynecological cancer. This cell line will not only contribute to elucidation of its pathogenesis, but also provide a preclinical model for drug discovery, accelerating both basic and translational research in gynecological cancer.

ACKNOWLEDGMENTS

We thank N. Sakurai, K. Takahashi, and N. Miyazawa for their technical assistance. We thank members of the Division of Oncogenomics and Division of Surgical Pathology at Chiba Cancer

Center for their support in genomic analyses and pathological examination and diagnosis, respectively. This work was supported in part by Chiba Prefecture Research Grants and KAKENHI (17K19624, 18K16823, and 19K09816) by the Japan Society for the Promotion of Science.

CONFLICT OF INTEREST

The authors have no conflict of interests.

ORCID

Yoshitaka Hippo  <https://orcid.org/0000-0002-4975-1812>

REFERENCES

1. Yamagami W, Nagase S, Takahashi F. Clinical statistics of gynecologic cancers in Japan. *Journal of Gynecologic Oncology*. 2017;28(2):e32.
2. Small W Jr, Bacon MA, Bajaj A, et al. Cervical cancer: a global health crisis. *Cancer*. 2017;123(13):2404-2412.
3. Cohen PA, Jhingran A, Oaknin A, Denny L. Cervical cancer. *Lancet (London, England)*. 2019;393(10167):169-182.
4. Loureiro J, Oliva E. The spectrum of cervical glandular neoplasia and issues in differential diagnosis. *Arch Pathol Lab Med*. 2014;138(4):453-483.
5. Seki H, Takada T, Sodemoto T, Hoshino H, Saitoh K, Uekusa T. A young woman with clear cell adenocarcinoma of the uterine cervix. *Int J Clin Oncol*. 2003;8(6):399-404.
6. Yabushita H, Kanyama K, Sekiya R, Noguchi M, Wakatsuki A. Clear-cell adenocarcinoma of the uterine cervix in a 17-year-old adolescent. *Int J Clin Oncol*. 2008;13(6):552-554.
7. Tantitamit T, Hamontri S, Rangsiratanakul L. Clear cell adenocarcinoma of the cervix in second generation young women who are without maternal exposure to diethylstilbestrol: a case report. *Gynecol Oncol Rep*. 2017;20:34-36.
8. Nakamura K, Nakayama K, Minamoto T, et al. Lynch syndrome-related clear cell carcinoma of the cervix: a case report. *Int J Mol Sci*. 2018;19(4):979.
9. Lee EK, Lindeman NI, Matulonis UA, Konstantinopoulos PA. POLE-mutated clear cell cervical cancer associated with in-utero diethylstilbestrol exposure. *Gynecol Oncol Rep*. 2019;28:15-17.
10. Jiang X, Jin Y, Li Y, et al. Clear cell carcinoma of the uterine cervix: clinical characteristics and feasibility of fertility-preserving treatment. *OncoTargets and Therapy*. 2014;7:111-116.
11. Huo D, Anderson D, Palmer JR, Herbst AL. Incidence rates and risks of diethylstilbestrol-related clear-cell adenocarcinoma of the vagina and cervix: update after 40-year follow-up. *Gynecol Oncol*. 2017;146(3):566-571.
12. Waggoner SE, Anderson SM, Van Eyck S, Fuller J, Luce MC, Herbst AL. Human papillomavirus detection and p53 expression in clear-cell adenocarcinoma of the vagina and cervix. *Obstet Gynecol*. 1994;84(3):404-408.
13. An HJ, Kim KR, Kim IS, et al. Prevalence of human papillomavirus DNA in various histological subtypes of cervical adenocarcinoma: a population-based study. *Mod Pathol*. 2005;18(4):528-534.
14. Kocken M, Baalbergen A, Sniijders PJ, et al. High-risk human papillomavirus seems not involved in DES-related and of limited importance in nonDES related clear-cell carcinoma of the cervix. *Gynecol Oncol*. 2011;122(2):297-302.

15. Sato T, Vries RG, Snippert HJ, et al. Single Lgr5 stem cells build crypt-villus structures in vitro without a mesenchymal niche. *Nature*. 2009;459(7244):262-265.
16. Sato T, Stange DE, Ferrante M, et al. Long-term expansion of epithelial organoids from human colon, adenoma, adenocarcinoma, and Barrett's epithelium. *Gastroenterology*. 2011;141(5):1762-1772.
17. Bartfeld S, Bayram T, van de Wetering M, et al. In vitro expansion of human gastric epithelial stem cells and their responses to bacterial infection. *Gastroenterology*. 2015;148(1):126-136.e6.
18. Chen YW, Huang SX, de Carvalho A, et al. A three-dimensional model of human lung development and disease from pluripotent stem cells. *Nat Cell Biol*. 2017;19(5):542-549.
19. Schumacher MA, Aihara E, Feng R, et al. The use of murine-derived fundic organoids in studies of gastric physiology. *J Physiol*. 2015;593(8):1809-1827.
20. Onuma K, Ochiai M, Orihashi K, et al. Genetic reconstitution of tumorigenesis in primary intestinal cells. *Proc Natl Acad Sci USA*. 2013;110(27):11127-11132.
21. Sato T, Morita M, Tanaka R, et al. Ex vivo model of non-small cell lung cancer using mouse lung epithelial cells. *Oncology Letters*. 2017;14(6):6863-6868.
22. Ochiai M, Yoshihara Y, Maru Y, et al. Kras-driven heterotopic tumor development from hepatobiliary organoids. *Carcinogenesis* 2019; [Epub ahead of print]. <https://doi.org/10.1093/carcin/bgz024>
23. Matsuura T, Maru Y, Izumiya M, et al. Organoid-based ex vivo reconstitution of Kras-driven pancreatic ductal carcinogenesis. *Carcinogenesis*. 2019; [Epub ahead of print]. <https://doi.org/10.1093/carcin/bgz122>
24. Boj SF, Hwang CI, Baker LA, et al. Organoid models of human and mouse ductal pancreatic cancer. *Cell*. 2015;160(1-2):324-338.
25. Li X, Francies HE, Secrier M, et al. Organoid cultures recapitulate esophageal adenocarcinoma heterogeneity providing a model for clonality studies and precision therapeutics. *Nat Commun*. 2018;9(1):2983.
26. Yan HHN, Siu HC, Law S, et al. A comprehensive human gastric cancer organoid biobank captures tumor subtype heterogeneity and enables therapeutic screening. *Cell Stem Cell*. 2018;23(6):882-97.e11.
27. Maru Y, Hippo Y. Current status of patient-derived ovarian cancer models. *Cells*. 2019;8(5):505.
28. Maru Y, Tanaka N, Itami M, Hippo Y. Efficient use of patient-derived organoids as a preclinical model for gynecologic tumors. *Gynecol Oncol*. 2019;154(1):189-198.
29. Maru Y, Onuma K, Ochiai M, Imai T, Hippo Y. Shortcuts to intestinal carcinogenesis by genetic engineering in organoids. *Cancer Sci*. 2019;110(3):858-866.
30. Maru Y, Tanaka N, Ohira M, Itami M, Hippo Y, Nagase H. Identification of novel mutations in Japanese ovarian clear cell carcinoma patients using optimized targeted NGS for clinical diagnosis. *Gynecol Oncol*. 2017;144(2):377-383.
31. Kobel M, Rahimi K, Rambau PF, et al. An Immunohistochemical Algorithm for Ovarian Carcinoma Typing. *Int J Gynecol Pathol*. 2016;35(5):430-441.
32. Pauli C, Hopkins BD, Prandi D, et al. Personalized in vitro and in vivo cancer models to guide precision medicine. *Cancer Discov*. 2017;7(5):462-477.
33. Sachs N, de Ligt J, Kopper O, et al. A living biobank of breast cancer organoids captures disease heterogeneity. *Cell*. 2018;172(1-2):373-86.e10.
34. Lee SH, Hu W, Matulay JT, et al. Tumor evolution and drug response in patient-derived organoid models of bladder cancer. *Cell*. 2018;173(2):515-28.e17.
35. Cancer Genome Atlas Research Network. Integrated genomic analyses of ovarian carcinoma. *Nature*. 2011;474(7353):609-615.
36. Reles A, Wen WH, Schmider A, et al. Correlation of p53 mutations with resistance to platinum-based chemotherapy and shortened survival in ovarian cancer. *Clin Cancer Res*. 2001;7(10):2984-2997.
37. Tiriach H, Belleau P, Engle DD, et al. Organoid profiling identifies common responders to chemotherapy in pancreatic cancer. *Cancer Discov*. 2018;8(9):1112-1129.
38. Kim HJ, Yoon A, Ryu JY, et al. c-MET as a potential therapeutic target in ovarian clear cell carcinoma. *Sci Rep*. 2016;6:38502.
39. Ochiai A, Takanashi A, Takekura N, et al. Establishment and characterization of cell line SFCC from clear cell adenocarcinoma of the uterine cervix. *Cancer*. 1989;64(4):854-859.
40. Koshiyama M, Matsumura N, Konishi I. Recent concepts of ovarian carcinogenesis: type I and type II. *Biomed Res Int*. 2014;2014:934261.
41. Kurman RJ, Shih IeM. The dualistic model of ovarian carcinogenesis: revisited, revised, and expanded. *Am J Pathol*. 2016;186(4):733-747.
42. Murakami R, Matsumura N, Brown JB, et al. Exome sequencing landscape analysis in ovarian clear cell carcinoma shed light on key chromosomal regions and mutation gene networks. *Am J Pathol*. 2017;187(10):2246-2258.
43. Yamamoto S, Tsuda H, Miyai K, Takano M, Tamai S, Matsubara O. Gene amplification and protein overexpression of MET are common events in ovarian clear-cell adenocarcinoma: their roles in tumor progression and prognostication of the patient. *Mod Pathol*. 2011;24(8):1146-1155.
44. Yamamoto S, Tsuda H, Miyai K, Takano M, Tamai S, Matsubara O. Accumulative copy number increase of MET drives tumor development and histological progression in a subset of ovarian clear-cell adenocarcinomas. *Mod Pathol*. 2012;25(1):122-130.
45. Lin HY, Huang CH, Wu WJ, Chang LC, Lung FW. TP53 codon 72 gene polymorphism paradox in associated with various carcinoma incidences, invasiveness and chemotherapy responses. *International Journal of Biomedical Science*. 2008;4(4):248-254.
46. Khan MH, Khalil A, Rashid H. Evaluation of the p53 Arg72Pro polymorphism and its association with cancer risk: a HuGE review and meta-analysis. *Genetics Research*. 2015;97:e7.
47. Storey A, Thomas M, Kalita A, et al. Role of a p53 polymorphism in the development of human papillomavirus-associated cancer. *Nature*. 1998;393(6682):229-234.
48. Dumont P, Leu JI, Della Pietra AC III, George DL, Murphy M. The codon 72 polymorphic variants of p53 have markedly different apoptotic potential. *Nat Genet*. 2003;33(3):357-365.
49. Lax SF, Kendall B, Tashiro H, Slebos RJ, Hedrick L. The frequency of p53, K-ras mutations, and microsatellite instability differs in uterine endometrioid and serous carcinoma: evidence of distinct molecular genetic pathways. *Cancer*. 2000;88(4):814-824.
50. Peng Y, Lin J, Guan J, et al. Ovarian collision tumors: imaging findings, pathological characteristics, diagnosis, and differential diagnosis. *Abdom Radiol*. 2018;43(8):2156-2168.

SUPPORTING INFORMATION

Additional supporting information may be found online in the Supporting Information section at the end of the article.

How to cite this article: Maru Y, Tanaka N, Ebisawa K, et al. Establishment and characterization of patient-derived organoids from a young patient with cervical clear cell carcinoma. *Cancer Sci*. 2019;110:2992-3005. <https://doi.org/10.1111/cas.14119>